Journal of Integrative Neuroscience

J. Integr. Neurosci. **2025**; 24(12): 43660
https://doi.org/10.31083/JIN43660

Original Research

From Silence to Awakening: The Role of Amplitude of Low-Frequency Fluctuations in Predicting Recovery After Spinal Cord Stimulation

Xuewei Qin[1,†], Xuanling Chen[1,†], Lan Yao[1,*], Hongchuan Niu[2], Kai Li[2], Yanli Lin[3], Shengpei Wang[4], Jiapeng Huang[5], Xiangyang Guo[6], Xiaoli Li[7]

[1]Department of Anesthesiology, Peking University International Hospital, 102206 Beijing, China
[2]Department of Neurosurgery, Peking University International Hospital, 102206 Beijing, China
[3]Department of Science and Education, Peking University International Hospital, 102206 Beijing, China
[4]Laboratory of Brain Atlas and Brain-Inspired Intelligence, Institute of Automation, Chinese Academy of Sciences, 100190 Beijing, China
[5]Department of Anesthesiology and Perioperative Medicine, University of Louisville, Louisville, KY 40202, USA
[6]Department of Anesthesiology, Peking University Third Hospital, 100191 Beijing, China
[7]State Key Laboratory of Cognitive Neuroscience and Learning & IDG/McGovern Institute for Brain Research, Beijing Normal University, 100875 Beijing, China
*Correspondence: yaolan@pkuih.edu.cn (Lan Yao)
[†]These authors contributed equally.

Academic Editor: Bettina Platt
Submitted: 11 June 2025 Revised: 30 October 2025 Accepted: 6 November 2025 Published: 25 December 2025

Abstract

Background: Disorders of consciousness (DoCs) following traumatic brain injury (TBI), or cerebrovascular disease (CVD) are difficult to prognose, as reliable biomarkers are lacking. Resting-state functional magnetic resonance imaging (fMRI) amplitude of low-frequency amplitude (ALFF) may capture etiology-specific neural activity, but its prognostic value for spinal cord stimulation (SCS) outcomes remains unknown. In this study we therefore investigated etiology-specific ALFF patterns in TBI- and CVD-induced DoCs and evaluated their prognostic value for recovery after SCS. **Methods**: Resting-state fMRI data from patients with TBI (n = 16) and CVD (n = 15), and healthy controls (n = 12), were analyzed. Whole-brain ALFF differences were also compared between the groups. Correlations between ALFF and 6-month post-SCS Coma Recovery Scale-Revised (CRS-R) score improvements were assessed. Logistic regression was used to identify consciousness recovery markers. **Results**: Compared with healthy controls, patients with TBI demonstrated a significant increase in ALFF within the bilateral insula, thalamus, and brainstem ($p < 0.05$), suggesting compensatory neural hyperactivity potentially involving glutamatergic pathways. Patients with CVD exhibited elevated ALFF in the contralateral sensorimotor cortex ($p < 0.05$), indicating ipsilateral neural reorganization. Notably, the thalamic ALFF were strongly correlated with consciousness recovery, as measured by improvements in CRS-R score at 6 months in both the TBI (r= 0.64, $p = 0.0071$) and CVD (r = 0.59, $p = 0.02$) groups. Furthermore, logistic regression analysis identified increased ALFF in the anterior cingulate cortex-thalamic loop (odds ratio [OR] = 3.21, $p < 0.05$) as a potential cross-etiology biomarker for recovery following SCS. **Conclusions**: ALFF reveal distinct neuroplasticity mechanisms, including compensatory activation in TBI and ipsilateral reorganization in CVD. Elevated anterior cingulate cortex (ACC)-thalamic ALFF are a key cross-etiology biomarker for consciousness recovery to guide SCS target selection.

Keywords: resting-state functional MRI; amplitude of low-frequency fluctuations; disorder of consciousness; spinal cord stimulation; neuroplasticity

1. Introduction

Disorders of consciousness (DoC) are a neurological consequence of severe brain injury, encompassing unresponsive wakefulness syndrome (UWS), minimally conscious state minus (MCS–), minimally conscious state plus (MCS+), and emergence from the minimally conscious state (EMCS). The pathological mechanisms underlying DoC involve extensive damage to the cortical–thalamic–brainstem networks [1–4]. In current clinical practice, diagnostic and prognostic evaluations primarily rely on behavioral scales such as the Coma Recovery Scale-Revised (CRS-R). However, functional neuroimaging has revealed behavioral misdiagnosis rates as high as 37% [5]. The limitations of these subjective assessments are attributed to three main factors: (i) motor deficits that hinder behavioral expression [6], (ii) fluctuations in consciousness that result in inconsistent assessment outcomes [7], and (iii) the presence of covert awareness undetectable using behavioral evaluations [8,9]. Therefore, the development of objective and quantitative neuromarkers is crucial for addressing these clinical challenges.

Resting-state functional magnetic resonance imaging (rs-fMRI) is a noninvasive method to elucidate spontaneous neural activity via blood oxygen level-dependent (BOLD) signals, offering a "neural window" for investigating the implicit networks associated with consciousness in patients with DoC. The amplitude of low-frequency fluctuation (ALFF), a fundamental metric of rs-fMRI, quanti-

fies the energy of BOLD oscillations within the 0.01–0.1 Hz frequency range. This physiological measure reflects the intensity of local neuronal metabolism, with increased ALFF indicating neural hyperactivity or compensatory activation and decreased ALFF suggesting functional inhibition or structural damage [10]. Owing to its sensitivity to local microloops, ALFF is considered a more appropriate metric for assessing DoC in cases of heterogeneous brain injury compared with network metrics such as functional connectivity (FC) [11]. In patients with traumatic brain injury (TBI), ALFF can reveal functional inhibition or compensatory activation within midbrain–thalamus–cortex loops, thereby reflecting neuronal overexcitation or reorganization following injury [10]. Conversely, patients who are comatose following resuscitation from cardiac arrest show increased mean whole-brain ALFF values, particularly in the left middle temporal and inferotemporal gyri. These elevated values are strongly correlated with cerebral oxygen saturation ($SjvO_2$) ($r = 0.910$), thereby offering direct quantification of the neurometabolic disturbances associated with hypoxic brain injury [12]. The sensitivity of ALFF has been validated in disorders such as schizophrenia, which shows increased ALFF in the inferior frontal gyrus and decreased ALFF in the cerebellum [13]. This finding supports the use of this method to assess localized microcircuits in various diseases. Research on the rehabilitation of motor function following brain injury suggests that modified constraint-induced movement therapy (mCIMT) promotes functional reorganization by modulating ALFF values in the motor cortex and thalamus. Moreover, these alterations are directly correlated with the degree of motor recovery [14].

Etiology-specific patterns of neural activity may significantly impact prognosis. TBI-induced DoC is characterized by diffuse axonal injury (DAI), which disrupts global brain connectivity, particularly affecting core nodes such as the default mode network (DMN), executive control network, and bilateral anterior cingulate gyrus within the salience networks [15,16]. In contrast, DoC resulting from cerebrovascular disease (CVD), such as those caused by basilar artery stroke, predominantly lead to damage to the thalamic and brainstem nuclei, which are essential for arousal regulation. This damage hinders the normal functioning of these nuclei and facilitates arousal [17]. Disruption of the thalamocortical loops and the upstream reticular activating system of the brainstem by these critical nuclei results in impaired arousal function [17]. Although recovery rates are higher in patients with TBI-induced DoC (38–78% at 1 year) compared with those with CVD-induced DoC (17%) [17,18], the neurofunctional basis for distinguishing this difference using rs-fMRI biomarkers remains poorly understood.

Spinal cord stimulation (SCS) has demonstrated promising clinical potential for the management of patients with DoC, particularly those with UWS and posttraumatic secondary severe DoC. SCS enhances consciousness and facilitates neurological recovery [19–21]. Short-term minimally invasive SCS (st-SCS) offers an improved balance between therapeutic efficacy and surgical risk, ensures greater safety, and is deemed suitable for treating patients with prolonged chronic DoC (pDOC) [22,23]. Mechanistically, SCS is hypothesized to modulate brain network activities such as enhancing cortical excitability and metabolic levels. This modulation can induce immediate alterations in electroencephalography (EEG) signals, which are closely associated with clinical prognosis and significant changes in cortical activity, as evidenced by combined transcranial magnetic stimulation (TMS-EEG) study [24]. Furthermore, high cervical SCS, including the "burst" stimulation mode, further enhances patient consciousness and reduces spasticity by modulating the brainstem–thalamus–cortex loop [20,25]. In practical applications, the integration of near-infrared spectroscopy (NIRS) with additional monitoring techniques facilitates the optimization of postoperative parameters and evaluation of treatment efficacy, thereby offering a crucial foundation for advancing personalized treatment approaches for SCS [25].

The present study aimed to delineate the differences in ALFF between patients with TBI and those with CVD using rs-fMRI. Additionally, this study sought to identify distinctive neural activity markers to predict recovery of consciousness following SCS.

2. Materials and Methods

2.1 Ethics Statement and Patient Selection

This study was approved by the Ethics Committee of Peking University International Hospital (2022-KY-0023-01) and complied with the tenets of the Declaration of Helsinki. All participants or their guardians provided written informed consent for participation and publication.

This study enrolled 35 patients with DoC and 12 healthy controls from the Department of Neurosurgery at Peking University International Hospital, all of whom underwent rs-fMRI and clinical evaluation. Patients with DoC were included if their illness lasted for >1 month, had no history of certain neurological disorders, had not used benzodiazepines 48 h before MRI, had no MRI contraindications, and had an intact cranial vault. Patients with insufficient injury type, poor rs-fMRI data, magnetic resonance imaging (MRI) contraindications, cranial defects, or refusal to participate were excluded from the study. Following the screening process, patients diagnosed with hypoxic-ischemic encephalopathy were also excluded due to the misalignment of this etiology with the study's primary focus on traumatic and cerebrovascular causes. Additionally, the sample size for a distinct hypoxic-ischemic group was deemed inadequate to conduct a meaningful analysis. The healthy control (HC) group included neurologically intact individuals without brain abnormalities recruited from patients scheduled for spinal surgery for intraspinal lesions.

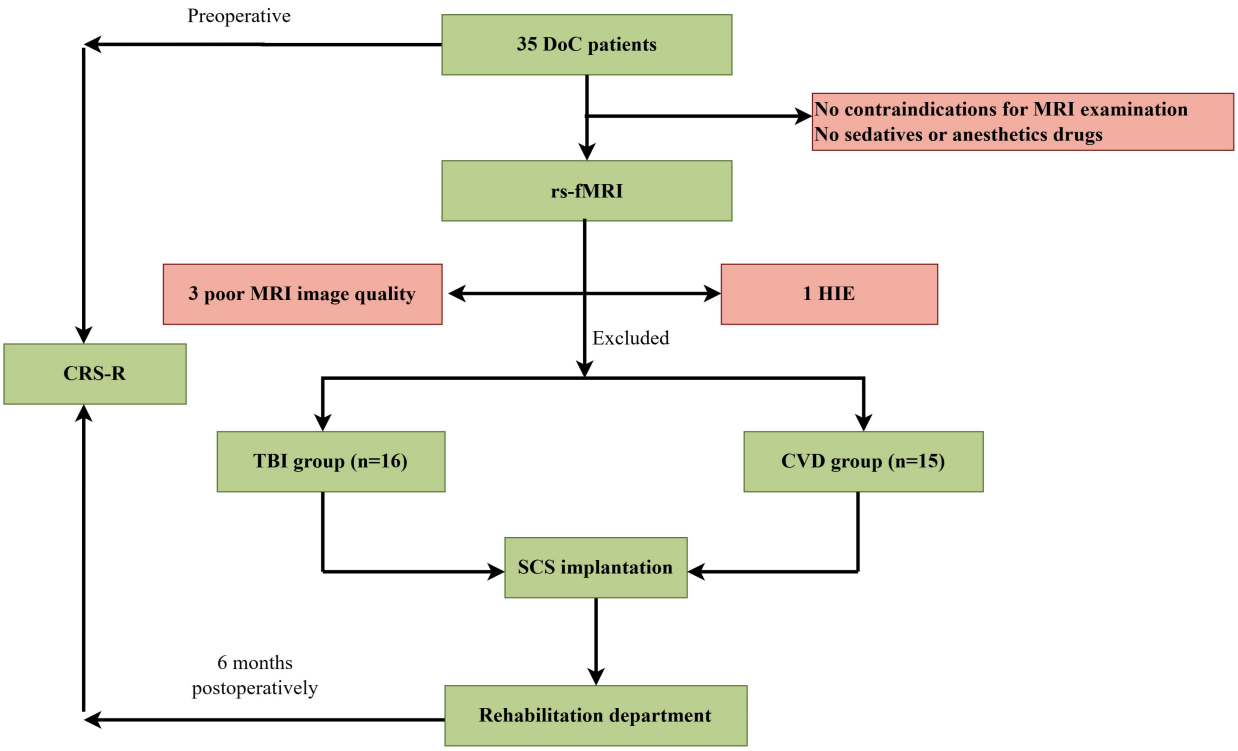

Fig. 1. Participant flow chart. DoC, disorders of consciousness; MRI, magnetic resonance imaging; rs-fMRI, resting-state functional MRI; HIE, hypoxic-ischemic encephalopathy; CRS-R, Coma Recovery Scale-revised; TBI, traumatic brain injury; CVD, cerebrovascular disease; SCS, spinal cord stimulation.

The inclusion criteria were American Society of Anesthesiologists (ASA) classification I–II, surgery for intraspinal lesions, absence of neurologic disease, no sedation within 48 h before surgery, and no contraindications to MRI. The exclusion criteria were severe cardiopulmonary disease, incomplete MRI data, history of cranial surgery, contraindications to MRI, difficulty in airway management, and refusal to participate in the study. The HC group comprised 12 patients with intradural lesions matched to the demographic characteristics of the study group, who underwent the same standardized rs-fMRI protocol.

Before the study, safety was ensured by checking vital signs, electrolyte levels, and blood counts according to clinical guidelines. Abnormal vital signs included systolic blood pressure >180 or <90 mmHg, diastolic pressure >110 or <60 mmHg, heart rate >100 or <50 bpm, oxygen saturation $<95\%$, or temperature >38 °C. Electrolyte imbalances (e.g., sodium <135 or >145 mmol/L, potassium <3.5 or >5.0 mmol/L) and abnormal blood counts (e.g., hemoglobin <10 g/dL, platelets $<100 \times 10^3/\mu$L) were flagged. Patients with abnormal values were excluded from scanning and were referred for further evaluation. Patients with DoC underwent tracheotomies, were off ventilatory support before the study, and received SCS to enhance wakefulness. A board-certified neurosurgeon with extensive experience with DoC evaluation conducted the CRS-R assessments before and 6 months after surgery. To reduce bias, the rater was blinded to the patients' ALFF and group allocation (TBI vs. CVD) during both assessments. Fig. 1 illustrates the study flowchart.

2.2 SCS Protocol

All enrolled patients underwent SCS. Under general anesthesia, a four-contact electrode was surgically implanted into the epidural space with the tip positioned at the midline of the C2–C4 segments of the cervical spinal cord. Postoperatively, an external pulse generator was connected to facilitate stimulation. The stimulation parameters were: 5/70 Hz frequency, 210 µs pulse width, and a stimulation intensity adjusted to slightly below the sensory threshold, typically 2–4 V [26]. Stimulation was administered in a cyclic mode consisting of 5 min of stimulation, followed by a 15-min rest interval. The total duration of daily stimulation was 8 h, and the treatment was sustained for 3–4 weeks. The efficacy of the intervention was evaluated weekly during the treatment period using the CRS-R.

2.3 Data Acquisition

The technician positioned the patient in the supine position on an MRI scanning bed. A foam pad was positioned within a coil to stabilize the patient's head and prevent movement. fMRI scanning was conducted using a 3.0 T MRI scanner (Magnetom Verio, software version syngo MR Dot; Siemens Healthineers, Munich, Germany)

equipped with eight phase-sensitive coding head coils. The parameters for structural imaging were as follows: repetition time (TR) = 2200 ms, echo time (TE) = 3.25 ms, inversion time = 900 ms, flip angle (FA) = 9°, field of view (FOV) = 250 × 250 mm, and matrix size = 256 × 256, with 192 slices and a slice thickness of 1.0 mm, without interslice spacing. For functional imaging, a gradient-echo planar imaging (EPI) sequence was employed with TR = 2220 ms, TE = 30 ms, FA = 90°, FOV = 192 × 192 mm, and a matrix size of 64 × 64. Functional images were acquired in the same orientation as the structural images, with 32 time points collected over a total duration of 540 s.

The data preprocessing involved converting the Digital Imaging and Communications in Medicine (DICOM) format to the Neuroimaging Informatics Technology Initiative (NIFTI) format, which necessitated the exclusion of the initial ten time-point signals to mitigate the influence of non-equilibrium magnetization effects. Additionally, temporal alignment and head-motion correction were performed, with the rejection criteria set at translations >3 mm and rotations >3°. The data were spatially normalized to the standard Montreal Neurological Institute (MNI) space using segmentation parameters, and voxel dimensions were resampled to a resolution of 3 × 3 × 3 mm^3. Spatial smoothing was performed using a Gaussian kernel with a full width at half-maximum (FWHM) of 4 mm. A band-pass filter with a frequency range of 0.01–0.08 Hz was employed for temporal filtering. Furthermore, the confounding effects of global signals, 24 head motion parameters, cerebrospinal fluid, and white matter signals were regressed using a linear regression approach. Global signal regression (GSR) was implemented to address the potential confounding influences of non-neuronal signals, such as global physiological noise and scanner drift. This method is widely and effectively utilized in rs-fMRI research on DoC to enhance the specificity of local neural activity estimations, as global signal fluctuations tend to be particularly prominent in this patient cohort [27].

2.4 ALFF Data Preprocessing

Initially introduced by Zang *et al.* [28] in 2007, ALFF is a well-established metric for quantifying spontaneous neural activity in rs-fMRI. This measure evaluates the total power within the typical low-frequency range (0.01–0.1 Hz) of the BOLD signal, thereby reflecting the intensity of regional neuronal activity. Although subsequent modifications, such as fractional ALFF (fALFF) and percent amplitude of fluctuation (PerAF), have been developed to enhance signal specificity or normalization, the present study used conventional ALFF because of its proven sensitivity in detecting localized neural hyperactivity and compensatory mechanisms in DoC [29,30]. This selection was consistent with our objective of capturing broad-spectrum neural activity alterations without potential confounders introduced by ratio-based or normalized metrics.

2.5 Region of Interest (ROI) Analysis of the Anterior Cingulate Cortex (ACC)-Thalamic Loop

To rigorously assess the involvement of the ACC-thalamic loop in the recovery of consciousness, we defined two regions of interest (ROIs). The ACC ROI was delineated as Brodmann areas 24 and 32, centered at Montreal Neurological Institute (MNI) coordinates (0, 42, 3), with a spherical radius of 6 mm. The thalamic ROI was defined using a bilateral thalamic mask obtained from the Automated Anatomical Labeling 3 (AAL3) atlas. For each participant, mean ALFF values within these ROIs were extracted and compared across groups (TBI, CVD, and HC) using one-way analysis of variance (ANOVA) followed by post-hoc t-tests. Additionally, correlation analyses were conducted to examine the relationship between ACC-thalamic ALFF and improvements in CRS-R scores.

2.6 Evaluation Criteria for Consciousness Improvement

The CRS-R assessed consciousness recovery prognosis in DoC patients. Improvement was defined as UWS patients advancing to MCS, MCS+, or EMCS, and MCS patients progressing to MCS+ or EMCS by the study's end (Table 1) [31].

2.7 Statistical Analyses

Data were analyzed using Statistical software (IBM SPSS Statistics for Windows, version 26.0; IBM Corporation, Armonk, NY, USA). The Shapiro–Wilk test was used to assess normality. Normally distributed data are reported as mean ± SD and compared using *t*-tests, while non-normally distributed data are shown as medians (interquartile range [IQR]) and compared using the Mann–Whitney U or Kruskal–Wallis H tests. Categorical data are presented as frequencies (%) and were analyzed using chi-squared or Fisher's exact tests. Whole-brain ALFF comparisons between the TBI, CVD, and HC groups were conducted using a voxel-wise general linear model. To address the risk of type I errors from multiple comparisons, statistical maps were corrected using the false discovery rate (FDR) method at $p < 0.05$. Only regions that passed this correction were considered significant. For hypothesis-driven correlation and regression analyses targeting specific regions such as the thalamus, a two-sided significance level of $p < 0.05$ was used. For whole-brain ALFF comparisons, Gaussian random field (GRF) correction was applied at the cluster level with a voxel-level threshold of $p < 0.001$ and a cluster-level threshold of $p < 0.05$, to correct for multiple comparisons.

This may have limited the statistical power of our analyses. A post-hoc power analysis for the primary correlation findings (thalamic ALFF vs. CRS-R improvement) was conducted using G*Power (version 3.1.9.7, Heinrich Heine University, Düsseldorf, Germany). For the TBI group with an observed correlation coefficient of r = 0.64 ($\alpha = 0.05$, two-tailed), the statistical power was 0.99. For the CVD group with an observed correlation coefficient of r = 0.59,

Table 1. CRS-R rating scale auditory.

		Visual		Motor		Promotor/verbal function		Communication		Arousal	
Consistent movement to command	4	Object recognition	5	Functional object use	6	Intelligible verbalization	3	Functional: Accurate	2	Attention	3
Reproducible movement to command	3	Object localization: Reaching	4	Automatic motor response	5	Vocalization/oral movement	2	Non-functional: intentional	1	Eye-opening without stimulation	2
Localization to sound	2	Pursuit eye movements	3	Object manipulation	4	Oral reflexive movement	1	None	0	Eye-opening with stimulation	1
Auditory startle	1	Fixation	2	Localization to noxious stimulation	3	None	0			None	0
None	0	Visual Startle	1	Flexion withdrawal	2						
		None	0	Abnormal posturing	1						
				None	0						
				UWS	MCS	EMCS					

The background colors in the table represent different levels of consciousness: white indicates UWS, light blue indicates MCS, and dark blue indicates EMCS. CRS-R, revised Coma Recovery Scale; UWS, unresponsive wakefulness syndrome; MCS, minimally conscious state; EMCS, emergence from the minimally conscious state.

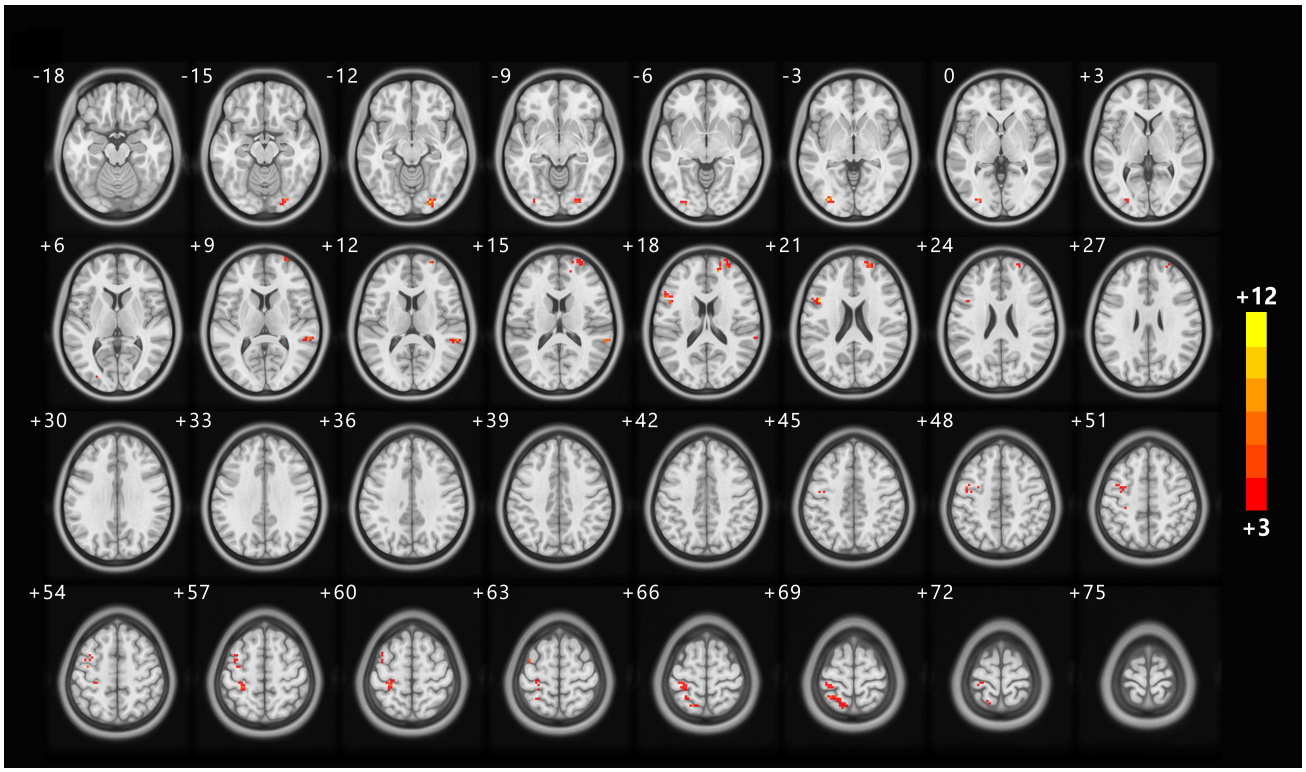

Fig. 2. Comparison of increased ALFF values between the TBI and HC groups. The TBI group showed higher ALFF values than the HC group in the Postcentral_L, Calcarine_R, Right Brainstem, Thalamus_R, Temporal_Inf_L, and Thalamus_L, with elevated regions marked in red (FDR-corrected, $p < 0.05$). ALFF, amplitude of low-frequency amplitude; HC, healthy control.

the power was 0.87. These results indicate that the primary correlations were detected with sufficient power, despite the modest sample sizes. However, for whole-brain voxel-wise comparisons and subgroup analyses, the power may be lower. Therefore, findings related to specific brain regions other than the thalamus should be interpreted as preliminary and require validation in larger cohorts.

Although the sample size for the logistic regression analysis (n = 31 for the TBI and CVD groups) was similar to that of previous neuroimaging study [10], it was still small for multivariate predictive modeling, potentially affecting the generalizability and stability of the results and requiring validation in larger, independent cohorts.

3. Results

3.1 Patient Demographics

Sex, age, disease duration, CRS-R score, and other subsets did not differ significantly between the TBI and CVD groups ($p > 0.05$). The HC group was also matched with the TBI and CVD groups in terms of sex and age ($p > 0.05$) (Table 2).

3.2 Lesion Characteristics

Analysis of the structural images revealed distinct lesion patterns consistent with the etiology. All patients in the TBI group exhibited neuroimaging features of diffuse axonal injury with common involvement of the corpus callosum (14/16, 87.5%), brainstem (9/16, 56.3%), and frontal white matter (12/16, 75.0%). In the CVD group, the lesions were primarily localized in the brainstem (10/15, 66.7%) and thalamus (8/15, 53.3%) and resulted from basilar artery occlusion or hemorrhage. Table 3 provides a detailed summary of the lesion locations. These structural differences provide an anatomical basis for interpreting subsequent ALFF alterations. This study used structural MRI to identify each patient's dominant lesion hemisphere. In the CVD group, patients had unilateral or mainly unilateral lesions, defining the "lesion hemisphere" as the side with more damage and the "contralateral hemisphere" as the less affected side. For the TBI group, where injuries were mostly bilateral, the "contralateral/ipsilateral" terms were not used; instead, comparisons were made using whole-brain ALFF maps.

3.3 Comparison of ALFF Values Between the TBI and HC Groups

Following FDR correction ($p < 0.05$), compared with the HC group, the TBI cohort exhibited significantly elevated ALFF values in the left postcentral (Postcentral_L), right calcarine (Calcarine_R), right brainstem (Right Brainstem), right thalamus (Thalamus_R), left inferior temporal gyrus (Temporal_Inf_L), and left thalamus (Thalamus_L) and significantly reduced val-

Table 2. Demographic characteristics of the three patient groups.

		Score	TBI group (n = 16)	CVD group (n = 15)	HC group (n = 12)	*p*
Age (years)			49.94 ± 10.87	47.87 ± 6.35	50.75 ± 10.22	0.704
Sex	M		6 (37.50%)	3 (20.00%)	5 (41.67%)	0.502
	F		10 (62.50%)	12 (80.00%)	12 (58.33%)	
Disease course (months)			3 (2.5, 5)	5 (3, 6.5)	4 (2.25, 7.5)	0.648
Diagnosis	UWS		11 (68.75%)	9 (60.00%)	—	0.845
	MCS–		5 (31.25%)	5 (33.33%)	—	
	MCS+		0 (0.00%)	1 (6.67%)	—	
CRS-R total scores	(Preoperative)		7 (7, 8)	8 (6, 8)	—	1.000
	Audio	0	4 (25.00%)	2 (13.33%)	—	0.654
		1	12 (75.00%)	13 (86.67%)	—	
		2	0 (0.00%)	0 (0.00%)	—	
	Visual	0	2 (12.50%)	7 (46.67%)	—	0.233
		1	5 (31.25%)	2 (13.33%)	—	
		2	6 (37.50%)	4 (24.67%)	—	
		3	3 (18.75%)	2 (13.33%)	—	
	Motor	1	3 (18.75%)	4 (26.67%)	—	0.511
		2	12 (75.00%)	8 (53.33%)	—	
		3	1 (6.25%)	1 (6.67%)	—	
		5	0 (0.00%)	2 (13.33%)	—	
CRS-R sub-item	Oral motor/verbal function	0	0 (0.00%)	0 (0.00%)	—	0.101
		1	16 (100.00%)	12 (80.00%)	—	
		2	0 (0.00%)	3 (20.00%)	—	
	Communication	0	16 (100.00%)	15 (100.00%)	—	1.000
		1	0 (0.00%)	0 (0.00%)	—	
		2	0 (0.00%)	0 (0.00%)	—	
	Arousal	0	1 (6.25%)	0 (0.00%)	—	1.000
		1	1 (6.25%)	1 (6.67%)	—	
		2	14 (87.50%)	13 (93.33%)	—	

CVD, cerebrovascular disease; TBI, traumatic brain injury; HC, healthy control; M, male; F, female.

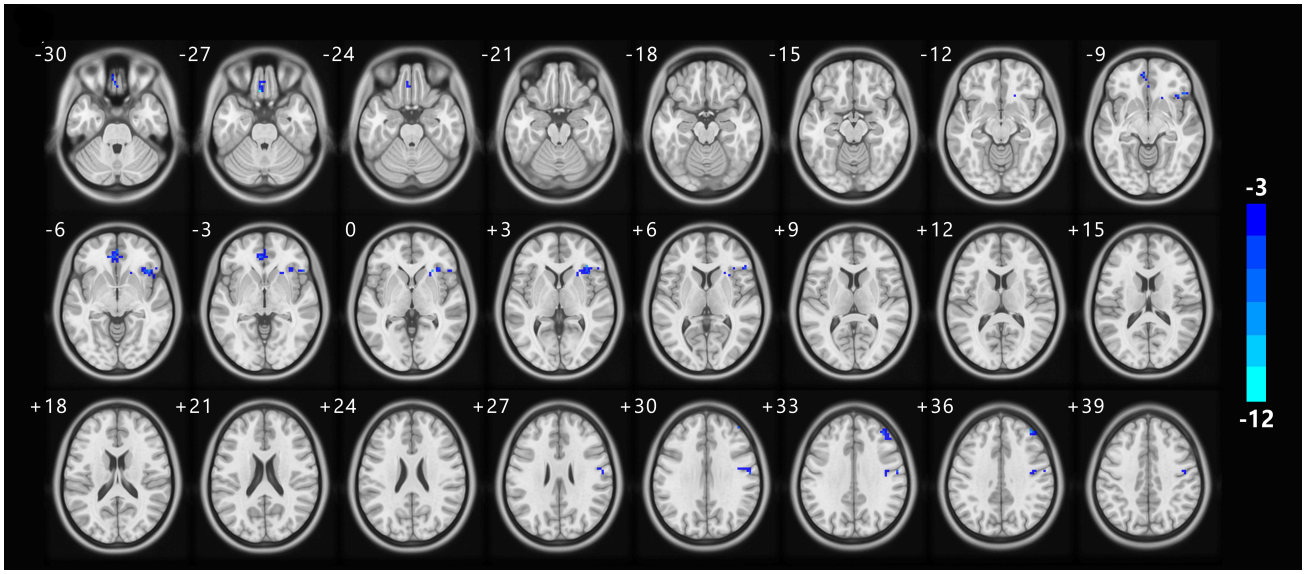

Fig. 3. Comparison of decreased ALFF values between the TBI and HC groups. Compared with the HC group, the TBI cohort demonstrated decreased ALFF values in several brain regions, including the Precuneus_R, Cingulum_Ant_L, Frontal_Sup_Orb_L, Occipital_Sup_R, Frontal_Sup_R, Rectus_R, Frontal_Sup_Orb_R, Hippocampus_R, and Frontal_Sup_Medial_L. Blue indicates brain regions with decreased values (FDR-corrected, $p < 0.05$).

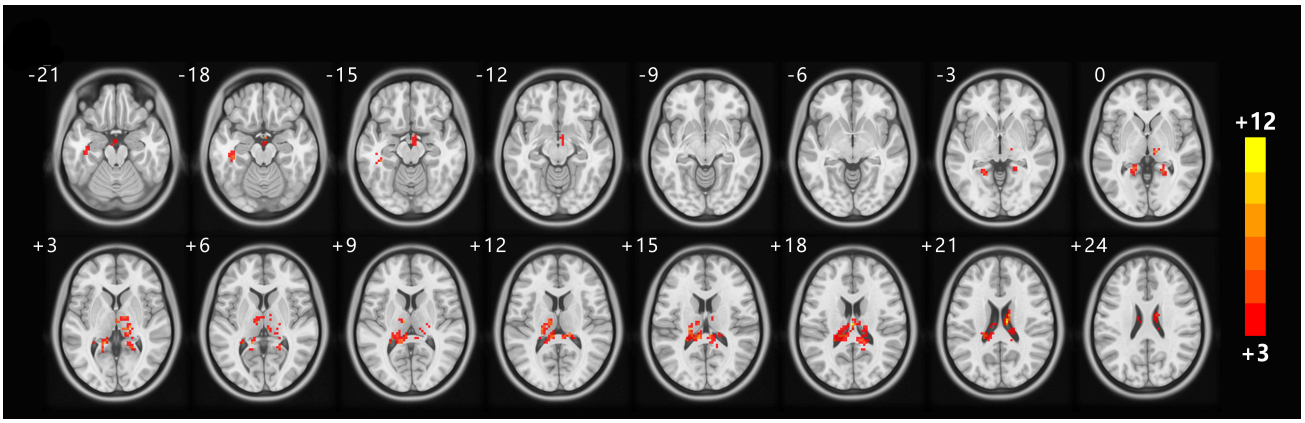

Fig. 4. Comparison of increased ALFF values between the CVD and HC groups. Compared with the HC group, the CVD cohort shows increased ALFF values in several brain regions, including Precentral_L, Parietal_Sup_L, Frontal_Sup_R, Temporal_Sup_R, Lingual_R, Frontal_Inf_Oper_L, Frontal_Inf_Oper_L, and Middle Occipital Gyrus L. Regions exhibiting elevated ALFF values are highlighted in red (FDR-corrected, $p < 0.05$).

Table 3. Summary of lesion locations in patients with TBI and CVD.

Lesion Location	TBI group (n = 16)	CVD group (n = 15)	*p*
Frontal lobe	12 (75.0%)	2 (13.3%)	0.001
Temporal lobe	8 (50.0%)	3 (20.0%)	0.086
Parietal lobe	7 (43.8%)	1 (6.7%)	0.020
Occipital lobe	5 (31.3%)	0 (0.0%)	0.021
Corpus callosum	14 (87.5%)	0 (0.0%)	0.000
Thalamus	6 (37.5%)	8 (53.3%)	0.384
Brainstem	9 (56.3%)	10 (66.7%)	0.558
Cerebellum	4 (25.0%)	2 (13.3%)	0.419

Data are presented as the number of patients (percentage). Patients often presented with lesions at multiple locations.

ues in the right precuneus (Precuneus_R), left anterior cingulate cortex (Cingulum_Ant_L), left orbital superior frontal gyrus (Frontal_Sup_Orb_L), right superior occipital gyrus (Occipital_Sup_R), right superior frontal gyrus (Frontal_Sup_R), right gyrus rectus (Rectus_R), right frontal superior occipital gyrus (Frontal_Sup_Orb_R), right hippocampus (Hippocampus_R), and left medial prefrontal cortex (Frontal_Sup_Medial_L). All significant regions are included in Table 4 and Figs. 2,3.

3.4 Comparison of ALFF Values Between the CVD and HC Groups

After applying FDR correction with a significance threshold of $p < 0.05$, compared with the HC group, the CVD group demonstrated significantly increased ALFF values in the left precentral gyrus (Precentral_L), left superior parietal lobule (Parietal_Sup_L), Frontal_Sup_R, right superior temporal gyrus (Temporal_Sup_R), right lingual gyrus (Lingual_R), left inferior frontal gyrus (Frontal_Inf_Oper_L), and Middle Occipital Gyrus L regions and significant decreases in the left rectus (Rectus_L), Left Inferior Frontal Gyrus, Orbital Part (Frontal_Inf_Orb_L), right middle frontal gyrus (Frontal_Mid_R), right insula (Insula_R), and Cingulum_Ant_L, (Table 5, Figs. 4,5).

3.5 Changes in Consciousness State in Patients With DoC 6 Months Postoperatively

The CVD and TBI groups had similar preoperative CRS-R scores (median = 7), which met the criteria for severe chronic DoC. Four (12.9 %) patients transitioned from MCS to EMCS. Six months postoperatively, consciousness improved in 60% of patients with CVD and 43.75% of patients with TBI, with no significant difference ($p = 0.479$) (Fig. 6A,B).

3.6 ALFF Alterations in the ACC-Thalamic Loop Across Etiologies

We analyzed the alterations in the ALFF within the predefined ACC-thalamic circuit, which is associated with arousal and conscious processing. Relative to healthy controls, both the TBI and CVD cohorts exhibited significantly increased ALFF in the thalamic ROI (TBI: $t = 4.92$, $p < 0.001$; CVD: $t = 3.45$, $p = 0.002$). Within the ACC ROI, compared with the HC group, significantly increased ALFF was observed in the TBI group ($t = 3.78$, $p < 0.001$), but not

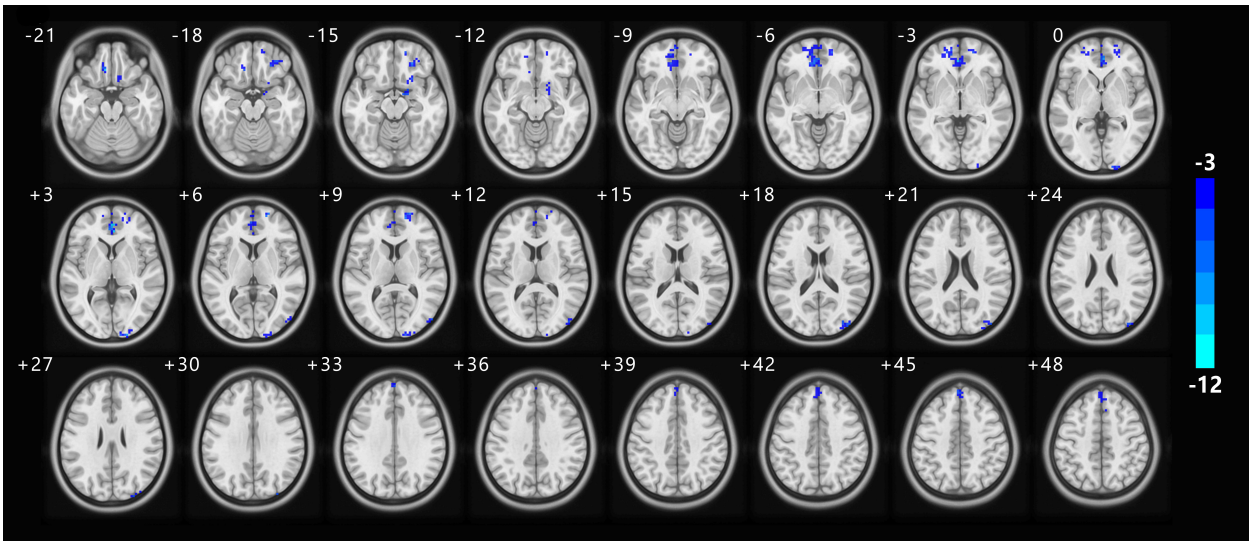

Fig. 5. Comparison of decreased ALFF values between the CVD and HC groups. Compared with the HC group, the CVD cohort showed decreased ALFF values in several brain regions, including the Rectus_L, Frontal_Inf_Orb_L, Frontal_Mid_R, Insula_R, and Cingulum_Ant_L. Blue indicates reduced brain regions (FDR-corrected, $p < 0.05$).

Table 4. Brain regions showing significant ALFF differences between the TBI and HC groups after FDR correction.

ALFF value change	Encephalic region	MNI space coordinates			Voxel number	T-value of the extreme point
		X	Y	Z		
Increase	Postcentral_L	–33	–36	66	29	4.3281
	Calcarine_R	21	–48	6	27	5.4853
	Right Brainstem	3	–3	–18	25	5.7182
	Thalamus_R	18	–21	3	97	7.4219
	Temporal_Inf_L	–33	–13	–24	33	7.7457
	Thalamus_L	0	–18	18	255	9.4179
Decrease	Precuneus_R	0	–48	60	29	–9.0652
	Cingulum_Ant_L	0	48	3	162	–7.3782
	Frontal_Sup_Orb_L	–9	30	–21	25	–7.0064
	Occipital_Sup_R	21	–102	3	32	–6.5780
	Frontal_Sup_R	21	63	6	20	–6.2167
	Rectus_R	9	18	–27	21	–5.8942
	Frontal_Sup_Orb_R	15	54	–15	31	–4.9527
	Hippocampus_R	15	–3	–15	22	–4.4328
	Frontal_Sup_Medial_L	0	57	33	66	–3.7859

ALFF, amplitude of low-frequency fluctuations; MNI, Montreal Neurological Institute; Postcentral_L, left postcentral; Calcarine_R, right calcarine; Right Brainstem, right brainstem; Thalamus_R, right thalamus; Temporal_Inf_L, left inferior temporal gyrus; Thalamus_L, left thalamus; Precuneus_R, right precuneus; Cingulum_Ant_L, left anterior cingulate cortex; Frontal_Sup_Orb_L, left orbital superior frontal gyrus; Occipital_Sup_R, right superior occipital gyrus; Frontal_Sup_R, right superior frontal gyrus; Rectus_R, right gyrus rectus; Frontal_Sup_Orb_R, right frontal superior occipital gyrus; Hippocampus_R, right hippocampus; Frontal_Sup_Medial_L, left medial prefrontal cortex.

the CVD group ($p = 0.12$). The combined ALFF values for the ACC-thalamic circuit (calculated as the mean of both ROIs) were significantly increased in both patient groups compared with the HC group (TBI: $p < 0.001$; CVD: $p = 0.003$), underscoring its relevance across etiologies. Spatial representations of the differences in ALFF within the ACC-thalamic circuit are shown in Fig. 7.

3.7 Comparison of Thalamic ALFF and CRS-R Correlation Between Patients With Enhanced Consciousness and HCs

Correlation analysis revealed a significant positive association between thalamic ALFF changes and CRS-R score improvements in patients with TBI (r = 0.64, $p = 0.0071$) and CVD (r = 0.59, $p = 0.02$), with a stronger association observed in the TB group. This finding suggests that

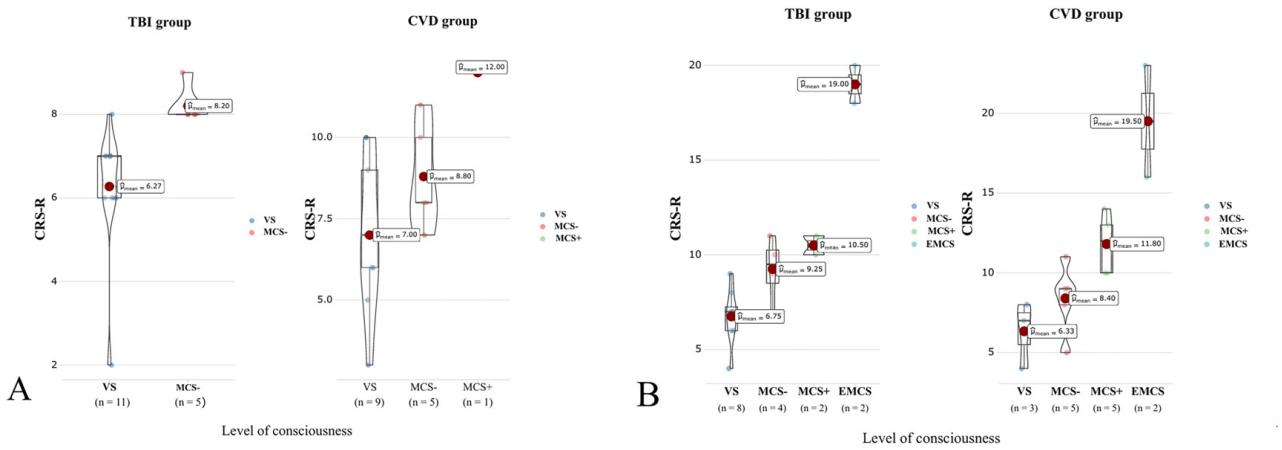

Fig. 6. Consciousness assessment by etiology. (A) Preoperatively. (B) 6 months post-operatively. The horizontal axis indicates etiology, and the vertical axis displays CRS-R scores.

Table 5. Brain regions with ALFF differences between the CVD and HC groups after FDR correction.

ALFF value change	Encephalic region	MNI space coordinates			Voxel numbers	T-value of the extreme point
		X	Y	Z		
Increase	Precentral_L	–39	0	63	33	3.4512
	Parietal_Sup_L	–18	–60	66	30	5.2701
	Frontal_Sup_R	15	51	18	40	6.8753
	Temporal_Sup_R	60	–39	12	20	8.0236
	Lingual_R	24	–87	–12	23	8.7329
	Frontal_Inf_Oper_L	–45	12	21	20	9.2859
	Middle Occipital Gyrus L	–33	–84	–3	22	9.8528
Decrease	Rectus_L	–6	30	–27	27	–9.2561
	Frontal_Inf_Orb_L	–39	36	–9	28	–8.3348
	Frontal_Mid_R	39	42	36	21	–6.9327
	Insula_R	27	24	0	65	–6.7462
	Cingulum_Ant_L	–6	42	–3	37	–5.4783

Precentral_L, left precentral gyrus; Parietal_Sup_L, left superior parietal lobule; Temporal_Sup_R, right superior temporal gyrus; Lingual_R, right lingual gyrus; Frontal_Inf_Oper_L, left inferior frontal gyrus; Rectus_L, left rectus; Left Inferior Frontal Gyrus, Orbital Part (Frontal_Inf_Orb_L); Frontal_Mid_R, right middle frontal gyrus; Insula_R, right insul.

thalamic ALFF alterations are positively associated with recovery of consciousness in both TBI and CVD, particularly in patients with TBI (Fig. 8).

3.8 Correlations Between Post-operative CRS-R Sub-items and Thalamic ALFF

In the TBI group, the thalamic ALFF showed the strongest correlation with the arousal ($r = 0.78$, $p < 0.001$), followed by motor ($r = 0.69$, $p = 0.003$) and visual ($r = 0.62$, $p = 0.011$) subitems. Audio, oral motor/verbal function, and communication showed no significant correlations. In the CVD group, the thalamic ALFF was most correlated with motor function ($r = 0.65$, $p = 0.008$) and arousal ($r = 0.58$, $p = 0.022$), with no significant associations with the visual, audio, oral motor/verbal function, or communication subitems. The arousal and motor subitems were the only dimensions that were consistently significantly correlated with thalamic ALFF across both etiologies. However, patients with TBI showed a stronger correlation with arousal, compared with motor function in patients with CVD (Table 6).

4. Discussion

This study employed ALFF analysis of rs-fMRI data to investigate the neural mechanisms underlying consciousness disorders with varying etiologies. By applying a rigorous statistical threshold to whole-brain comparisons, we identified two distinct and robust neuroplasticity patterns associated with traumatic and cerebrovascular origins.

In patients with TBI, the markedly elevated ALFF observed in the bilateral insula, thalamus, and brainstem (refer to Table 4 and Fig. 2) indicates a compensatory neural hyperactivity. This extensive upregulation of local neural activity is likely a mechanism to sustain arousal and fun-

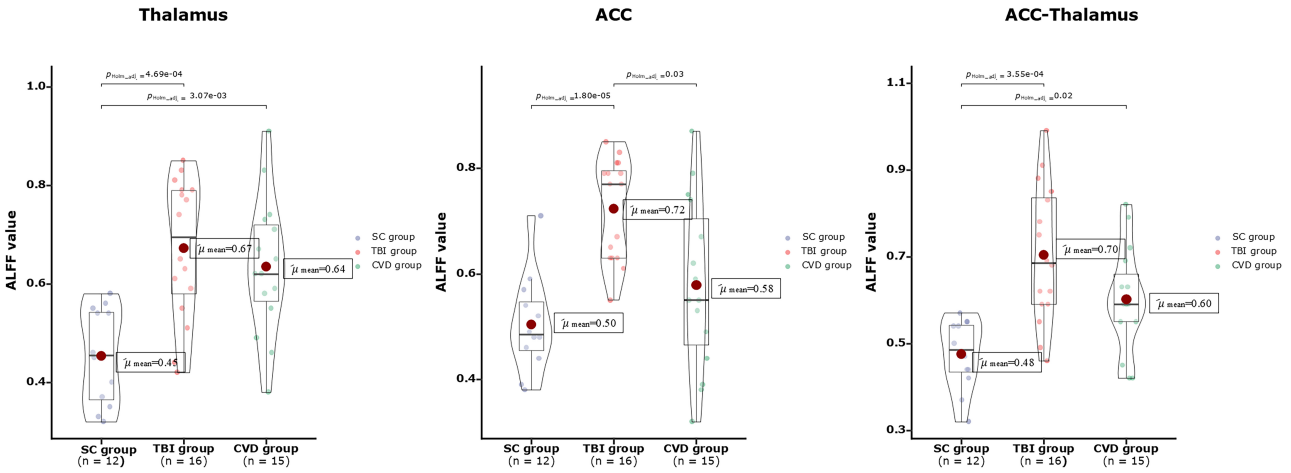

Fig. 7. Comparisons of ALFF values in key regions of interest among patient groups. Both the TBI and CVD groups exhibited increased ALFF in the thalamus and the integrated ACC-thalamus circuit when compared to HCs. However, ACC hyperactivity was observed only in the TBI group. The data are presented as mean ± standard error of the mean (SEM), and the *p*-values have been adjusted using the Holm–Bonferroni correction method. ACC, anterior cingulate cortex.

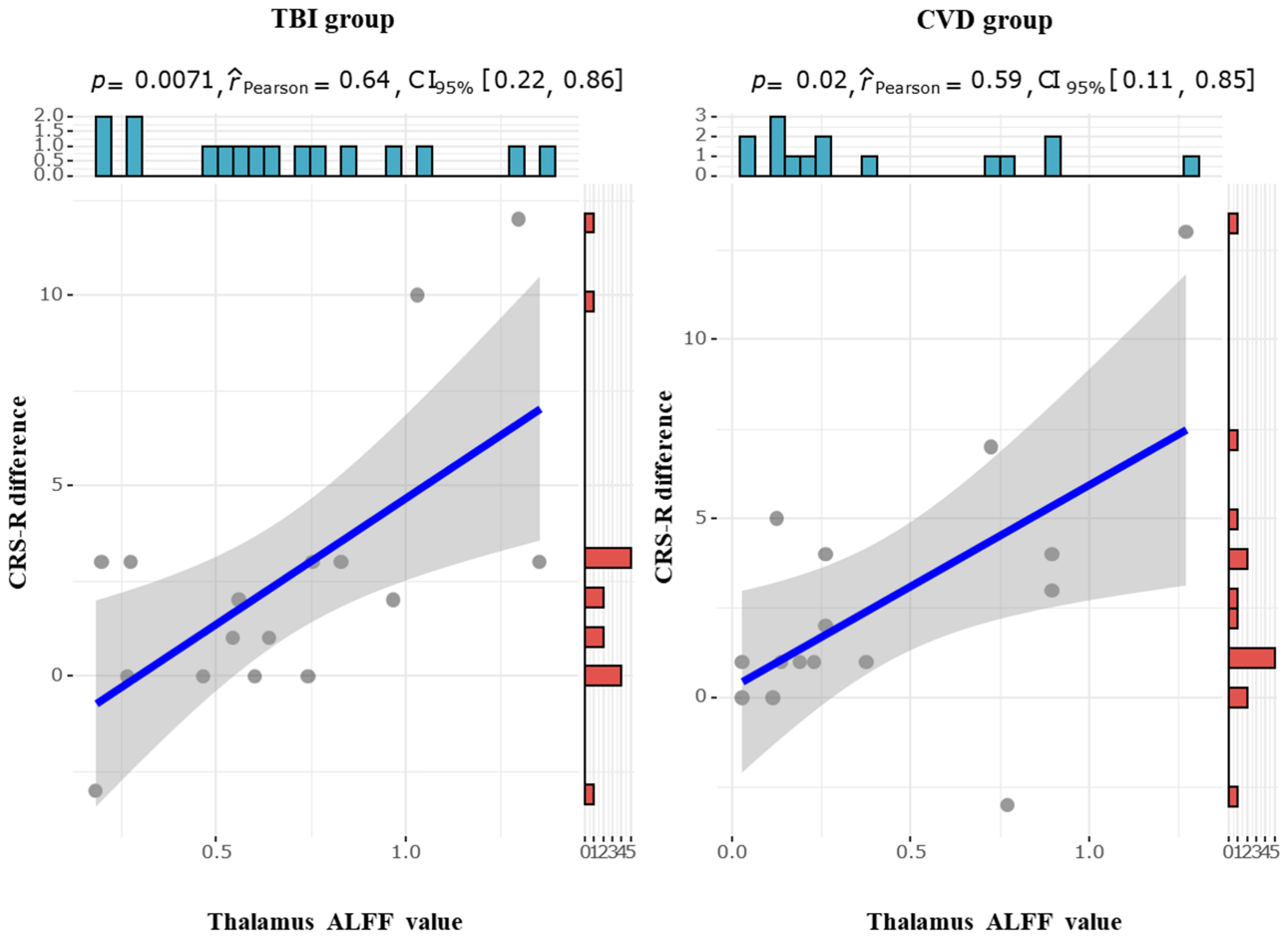

Fig. 8. Correlation between thalamic ALFF and CRS-R in two groups of patients with enhanced consciousness versus healthy controls. The TBI group shows a strong positive correlation (r = 0.64, $p = 0.0071$), while the CVD group shows a moderate correlation (r = 0.59, $p = 0.02$). This suggests that higher thalamic ALFF values are associated with better consciousness, with the TBI group showing a stronger correlation, highlighting differences in the impact of thalamic function recovery on consciousness between the two conditions.

Table 6. Correlations between thalamic ALFF and postoperative CRS-R sub-item improvements.

CRS-R Sub-item	TBI group (n = 16)		CVD group (n = 15)	
	r	*p*	r	*p*
Auditory	0.35	0.168	0.38	0.174
Visual	0.62	0.011	0.43	0.115
Motor	0.69	0.003	0.65	0.008
Oral	0.29	0.257	0.21	0.426
Motor/Verbal communication	0.08	0.752	0.15	0.589
Arousal	0.78	0.000	0.58	0.022

damental conscious processing amidst the widespread network disruption resulting from diffuse axonal injury [32–35]. The robust correlation between thalamic ALFF and arousal improvements (r = 0.78, Table 6) further highlights the functional significance of this compensatory mechanism in the recovery process. In contrast, in patients with CVD, the increased ALFF in the sensorimotor cortex contralateral to the primary lesion side (Precentral_L, Postcentral_L; see Table 5 and Fig. 4) illustrates the phenomenon of functional reorganization in the unaffected hemisphere. This observation aligns with the well-established concept that the unaffected hemisphere undergoes reorganization to compensate for focal subcortical lesions [36–38]. The significant positive correlation between sensorimotor ALFF and motor recovery (r = 0.52, $p = 0.03$) directly associates this reorganization pattern with enhanced behavioral outcomes, providing compelling evidence that functional migration to the intact hemisphere underlies motor recovery. In patients with CVD, structural MRI showed that lesions were not always on the left hemisphere. Of the 15 patients, 9 (60%) had primary lesions on the right side, mainly in the right brainstem and thalamus, while 6 (40%) had them on the left. The 'lesion hemisphere' was defined as the one with the most severe damage, assessed by two neuroradiologists using T1 and T2-weighted MRI, while the 'contralateral hemisphere' had minimal or no damage. Increased ALFF in the Precentral_L and Postcentral_L regions was linked to right-sided lesions, indicating functional reorganization in the left sensorimotor cortex. For left-sided lesions, increased ALFF was found in the right sensorimotor cortex (Precentral_R, Postcentral_R). However, these regions did not achieve statistical significance after FDR correction ($p = 0.08$ for both), likely due to the smaller sample size of this subgroup. This hemisphere-specific pattern substantiates that the observed elevation in sensorimotor ALFF represents a generalized contralateral reorganization response to focal subcortical lesions, rather than being specific to the left hemisphere.

In the TBI group, significant hyperactivity in the bilateral insula, thalamus, and brainstem may reflect compensatory neural mechanisms previously linked to alterations in glutamatergic neurotransmission in models of diffuse axonal injury [39–42]. The insula is a synaptic network hub, and its compensatory increase in ALFF may sustain basal arousal by facilitating the integration of internal sensory information with environmental cues [43–45]. Both TBI and post-traumatic stress disorder (PTSD) are associated with functional abnormalities in prefrontal-subcortical emotion regulation circuits. Furthermore, glucocorticoids released after acute-phase injury may overstimulate glutamatergic activity, particularly in these circuits [43]. This heightened neural activity could be associated with sustained arousal, potentially involving glutamatergic pathways [46]. Additionally, disruption of glutamatergic signaling pathways can impair synaptic function following TBI. Targeted interventions, such as glycyrrhizic acid, berberine, and rhein (GBR)-gel, may help restore these pathways and mitigate neurological deficits [47]. Abnormalities in insula-brainstem connectivity, such as diminished effective connectivity from the left cerebral tract to the insula, further support the hypothesis that alterations in activity may indicate functional compensatory mechanisms [48]. Conversely, a concurrent increase in thalamus-brainstem ALFF facilitates the reactivation of subcortical arousal pathways. Abnormal thalamocortical communication is a pivotal factor in consciousness [49]. Experimental investigations have demonstrated significantly weakened (reduced effective connectivity) connectivity from the thalamus, particularly the left thalamus, to the brainstem; however, heightened activity may offset this loss by augmenting glutamatergic signaling [50]. In animal models, inhibiting forebrain glutamatergic neuronal activity restores normal functioning of the brainstem–thalamic pathway and mitigates arousal deficits [51].

Moreover, our ROI-based analysis identified the ACC-thalamic loop as a region exhibiting consistently elevated ALFF across both TBI and CVD etiologies. This finding is consistent with the established role of the ACC-thalamic loop in integrating arousal and affective processing, thereby supporting its potential utility as a cross-etiology biomarker for predicting responses to SCS. In addition, the logistic regression model corroborated the association of a higher baseline ALFF within this loop with improved recovery outcomes. The CVD cohort demonstrated significantly increased ALFF within the Precentral_L, Postcentral_L, and Parietal_Sup_L on the side contralateral to the lesion, consistent with previous reports [52–54], and provide empirical support for the "ipsilateralized migration

of neurological functions" hypothesis [53,54]. This hypothesis proposes that the intact hemisphere compensates for cerebrovascular lesion-induced impairments, such as those resulting from basilar artery strokes, by assuming that the thalamic and brainstem arousal function through compensatory reorganization. The underlying pathology of this phenomenon is attributed to disruption of the thalamocortical loop [55–57] and the brainstem's upstream reticular activating system [17], both of which are essential for maintaining arousal. Consequently, the sensorimotor network is compelled to sustain its basal function through ipsilateral reorganization.

The principal finding in this study was that increased ALFF in the sensorimotor cortex was significantly positively correlated with enhanced motor-following behavior after SCS ($r = 0.52$, $p = 0.03$). This observation suggests that the recuperation of motor function in patients with CVD depends on the compensatory reorganization capacity of the intact hemisphere, thereby offering imaging evidence supporting the neural mechanism underlying SCS therapy. Although consciousness recovery rates were higher in the CVD group (60%) than in the TBI group (60% vs. 43.75%) at 6 months (Fig. 6B), the comparatively weaker correlation between thalamic ALFF and CRS-R ($r = 0.70$) suggests that cortical reorganization, rather than thalamic reactivation, plays a more significant role in recovery in patients with CVD.

Our findings demonstrated both convergent and divergent patterns of ALFF between patients with TBI and CVD, indicative of etiology-specific neuroplasticity mechanisms. The persistent increase in thalamic ALFF observed in both cohorts, along with its significant correlation with the recovery of consciousness, highlights the pivotal role of the thalamus in the regulation of arousal and integrative functions across different etiologies. This convergence implies that thalamic hyperactivity may be a common compensatory mechanism to maintain consciousness despite various structural injuries. In contrast, variable alterations in ALFF observed in other regions, such as increased activity in the insula and brainstem in TBI compared with contralateral sensorimotor cortex reorganization in CVD, underscore distinct pathophysiological mechanisms. In TBI, diffuse axonal injury disrupts extensive neural networks, leading to widespread compensatory glutamatergic activation in central hubs such as the insula and brainstem [58]. Conversely, in CVD, focal subcortical lesions (e.g., in the thalamus or brainstem) prompt ipsilateral cortical reorganization, particularly within sensorimotor regions, to compensate for impaired arousal pathways [59]. These findings indicate that while the thalamus functions as a universal hub for the recovery of consciousness, adaptive network responses are contingent on the underlying etiology. TBI involves diffuse compensatory activation, whereas CVD is characterized by focal cortical reorganization.

Correlation analysis of CRS-R sub-items and thalamic ALFF further refined the functional role of thalamic activity in the recovery of consciousness. The consistent association between thalamic ALFF and the arousal and motor sub-items in both the TBI and CVD groups suggests that the thalamus primarily modulates consciousness dimensions linked to arousal maintenance and motor output integration, two core components of conscious expression [60,61]. The stronger correlation with arousal in patients with TBI ($r = 0.78$ vs. $r = 0.58$ in CVD) may reflect the compensatory role of the thalamus in restoring basal arousal, in which TBI-induced diffuse axonal injury disrupts brainstem-thalamic arousal pathways [32,55]; elevated thalamic ALFF likely offsets this disruption by enhancing glutamatergic signaling [62,63], thereby improving arousal stability. In contrast, patients with CVD (with focal thalamic/brainstem lesions) showed a stronger correlation with motor function ($r = 0.65$ vs. $r = 0.69$ in TBI), consistent with the "ipsilateral reorganization" hypothesis suggesting that the thalamus may coordinate with the contralateral sensorimotor cortex (as observed in the increased ALFF in the CVD group) to facilitate motor recovery, a key behavioral marker of conscious improvement [64,65]. The lack of significant correlations with communication or oral motor/verbal function suggests that these higher-order cognitive dimensions may depend on additional networks (e.g., frontal-subcortical loops) rather than on isolated thalamic activity, consistent with prior findings that complex conscious behaviors require integrated cortical–thalamic–brainstem connectivity [66–68].

This study has some limitations. For instance, the modest sample sizes for the TBI ($n = 16$) and CVD ($n = 15$) groups limited the statistical power and increased the risk of overfitting in the logistic regression model for predicting consciousness recovery. Additionally, the interpretation of etiology-specific ALFF changes as compensatory mechanisms is correlative, and future studies with voxel-based lesion-symptom mapping (VLSM) or diffusion tensor imaging (DTI) are needed to potentially establish causal links. Moreover, relying solely on ALFF without multimodal functional connectivity may result in missing network-level dynamics. In addition, the 3 mm voxel resolution and head motion threshold (>3 mm/°) could have affected the detection of fine structures and data reliability. Also, the lack of a control group and follow-up beyond 1 year makes it difficult to separate treatment effects from natural recovery. When GSR was used, sensitivity analyses without GSR could confirm robustness, as prior evidence shows a limited impact on core ALFF patterns in patients with DoC [69,70]. Finally, the ACC-thalamic loop was defined using standard criteria; however, future studies could benefit from patient-specific connectivity mapping for greater precision. Larger multicenter studies are required to validate and generalize these findings.

5. Conclusions

The results of the current study identified distinct differences in the ALFF characteristics between DoC resulting from TBI and CVD based on analysis of rs-fMRI scans. Specifically, the TBI group showed compensatory activation in the insula and thalamus, whereas the CVD group showed reorganization in the contralateral sensorimotor areas. Additionally, a high ALFF in the anterior cingulate cortex-thalamic loop (>0.8, OR = 3.21) was initially identified as a possible biomarker for consciousness recovery across different causes. However, these findings require validation in larger studies.

Abbreviations

ACC, anterior cingulate cortex; ALFF, amplitude of low-frequency fluctuation; ANOVA, analysis of variance; ASA, American Society of Anesthesiologists; AAL3, Automated Anatomical Labeling 3; BOLD, blood oxygen level-dependent; ChiCTR, Chinese Clinical Trial Register; CRS-R, Coma Recovery Scale-Revised; CVD, cerebrovascular disease; DAI, diffuse axonal injury; DMN, default mode network; DoC, disorders of consciousness; EEG, electroencephalography; EMCS, emergence from the minimally conscious state; EPI, echo planar imaging; FA, flip angle; fALFF, fractional amplitude of low-frequency fluctuation; FDR, false discovery rate; FOV, field of view; FWHM, full width at half-maximum; GRF, Gaussian random field; GSR, global signal regression; HC, healthy control; HIE, hypoxic-ischemic encephalopathy; IQR, interquartile range; M, male; F, female; MCS, minimally conscious state; MCS-, minimally conscious state minus; MCS+, minimally conscious state plus; mCIMT, modified constraint-induced movement therapy; MNI, Montreal Neurological Institute; MRI, magnetic resonance imaging; NIRS, near-infrared spectroscopy; OR, odds ratio; pDOC, prolonged chronic disorder of consciousness; PerAF, percent amplitude of fluctuation; ROI, region of interest; rs-fMRI, resting-state functional magnetic resonance imaging; SCS, spinal cord stimulation; SD, standard deviation; $SjvO_2$, cerebral oxygen saturation; st-SCS, short-term spinal cord stimulation; TBI, traumatic brain injury; TE, echo time; TMS, transcranial magnetic stimulation; TR, repetition time; UWS, unresponsive wakefulness syndrome.

Availability of Data and Materials

To obtain the datasets used and analyzed in this study, please contact the corresponding author.

Author Contributions

Clinical data were acquired by XQ, XC, KL, YL and HN. Substantial contributions to the conception or design of the work by LY, JH, and XG. The initial draft of the manuscript was prepared by XQ and XC, while LY, JH, and XG provided critical revisions for significant intellectual content. Statistical analyses were executed by XQ, XC, SW and XL The study was supervised by LY, XG, and XL. All authors contributed to editorial changes in the manuscript. All authors read and approved the final manuscript. All authors have participated sufficiently in the work and agreed to be accountable for all aspects of the work.

Ethics Approval and Consent to Participate

The study was conducted in accordance with the Declaration of Helsinki. The research protocol was approved by the Ethics Committee of Peking University International Hospital (Ethic Approval Number: 2022-KY-0023-01), and all of the participants' guardians provided signed informed consent.

Acknowledgment

The authors express their gratitude to Professor Xuan Zhang for supplying the rs-fMRI data pertaining to patients with DoC.

Funding

The study was financially supported by the National Major Science and Technology Projects of China (STI2030-Major projects) (2021ZD0204304).

Conflict of Interest

The authors declare no conflict of interest.

Declaration of AI and AI-Assisted Technologies in the Writing Process

During the preparation of this work the authors used ChatGpt-3.5 in order to check spelling and grammar. After using this tool, the authors reviewed and edited the content as needed and takes full responsibility for the content of the publication.

References

[1] Mofakham S, Fry A, Adachi J, Stefancin PL, Duong TQ, Saadon JR, *et al*. Electrocorticography reveals thalamic control of cortical dynamics following traumatic brain injury. Communications Biology. 2021; 4: 1210. https://doi.org/10.1038/s42003-021-02738-2.

[2] Rosenzopf H, Klingbeil J, Wawrzyniak M, Röhrig L, Sperber C, Saur D, *et al*. Thalamocortical disconnection involved in pusher syndrome. Brain: a Journal of Neurology. 2023; 146: 3648–3661. https://doi.org/10.1093/brain/awad096.

[3] Toker D, Müller E, Miyamoto H, Riga MS, Lladó-Pelfort L, Yamakawa K, *et al*. Criticality supports cross-frequency cortical-thalamic information transfer during conscious states. eLife. 2024; 13: e86547. https://doi.org/10.7554/eLife.86547.

[4] Spindler LRB, Luppi AI, Adapa RM, Craig MM, Coppola P, Peattie ARD, *et al*. Dopaminergic brainstem disconnection is common to pharmacological and pathological consciousness perturbation. Proceedings of the National Academy of Sciences of the United States of America. 2021; 118: e2026289118. https://doi.org/10.1073/pnas.2026289118.

[5] Porcaro C, Marino M, Carozzo S, Russo M, Ursino M, Ruggiero V, *et al*. Fractal Dimension Feature as a Signature of Severity in Disorders of Consciousness: An EEG Study. International Journal of Neural Systems. 2022; 32: 2250031. https://doi.org/10.1142/S0129065722500319.

[6] Zheng RZ, Qi ZX, Wang Z, Xu ZY, Wu XH, Mao Y. Clinical Decision on Disorders of Consciousness After Acquired Brain Injury: Stepping Forward. Neuroscience Bulletin. 2023; 39: 138–162. https://doi.org/10.1007/s12264-022-00909-7.

[7] Liuzzi P, Hakiki B, Magliacano A, Chiesa G, De Bellis F, Cecchi F, *et al*. The Consciousness Domain Index: External Validation and Prognostic Relevance of a Data-Driven Assessment. IEEE Journal of Biomedical and Health Informatics. 2023; 27: 3559–3568. https://doi.org/10.1109/JBHI.2023.3264987.

[8] Amiri M, Fisher PM, Raimondo F, Sidaros A, Cacic Hribljan M, Othman MH, *et al*. Multimodal prediction of residual consciousness in the intensive care unit: the CONNECT-ME study. Brain: a Journal of Neurology. 2023; 146: 50–64. https://doi.org/10.1093/brain/awac335.

[9] Bodien YG, Allanson J, Cardone P, Bonhomme A, Carmona J, Chatelle C, *et al*. Cognitive Motor Dissociation in Disorders of Consciousness. The New England Journal of Medicine. 2024; 391: 598–608. https://doi.org/10.1056/NEJMoa2400645.

[10] Li C, Chen P, Deng Y, Xia L, Wang X, Wei M, *et al*. Abnormalities of cortical and subcortical spontaneous brain activity unveil mechanisms of disorders of consciousness and prognosis in patients with severe traumatic brain injury. International Journal of Clinical and Health Psychology: IJCHP. 2024; 24: 100528. https://doi.org/10.1016/j.ijchp.2024.100528.

[11] López-González A, Panda R, Ponce-Alvarez A, Zamora-López G, Escrichs A, Martial C, *et al*. Loss of consciousness reduces the stability of brain hubs and the heterogeneity of brain dynamics. Communications Biology. 2021; 4: 1037. https://doi.org/10.1038/s42003-021-02537-9.

[12] Shao R, Wang T, Hang C, An L, Wang X, Zhang L, *et al*. Alteration in early resting state functional MRI activity in comatose survivors of cardiac arrest: a prospective cohort study. Critical Care (London, England). 2024; 28: 260. https://doi.org/10.1186/s13054-024-05045-4.

[13] Zhang R, Ren J, Lei X, Wang Y, Chen X, Fu L, *et al*. Aberrant patterns of spontaneous brain activity in schizophrenia: A resting-state fMRI study and classification analysis. Progress in Neuro-psychopharmacology & Biological Psychiatry. 2024; 134: 111066. https://doi.org/10.1016/j.pnpbp.2024.111066.

[14] Sun CC, Zhang YW, Xing XX, Yang Q, Cao LY, Cheng YF, *et al*. Modified constraint-induced movement therapy enhances cortical plasticity in a rat model of traumatic brain injury: a resting-state functional MRI study. Neural Regeneration Research. 2023; 18: 410–415. https://doi.org/10.4103/1673-5374.344832.

[15] Qi Z, Zeng W, Zang D, Wang Z, Luo L, Wu X, *et al*. Classifying disorders of consciousness using a novel dual-level and dual-modal graph learning model. Journal of Translational Medicine. 2024; 22: 950. https://doi.org/10.1186/s12967-024-05729-z.

[16] Goodman AM, Kakulamarri P, Nenert R, Allendorfer JB, Philip NS, Correia S, *et al*. Relationship between intrinsic network connectivity and psychiatric symptom severity in functional seizures. Journal of Neurology, Neurosurgery, and Psychiatry. 2023; 94: 136–143. https://doi.org/10.1136/jnnp-2022-329838.

[17] Kowalski RG, Hammond FM, Weintraub AH, Nakase-Richardson R, Zafonte RD, Whyte J, *et al*. Recovery of Consciousness and Functional Outcome in Moderate and Severe Traumatic Brain Injury. JAMA Neurology. 2021; 78: 548–557. https://doi.org/10.1001/jamaneurol.2021.0084.

[18] Magyar-Sumegi ZD, Csendes M, Lendvai-Emmert D, Sebestyen G, Tamas V, Bandi S, *et al*. Chronic impairment of neurovascular coupling and cognitive decline in young survivors of severe traumatic brain injury. GeroScience. 2025; 10.1007/s11357–10.1007/s11357–025–01683–w. https://doi.org/10.1007/s11357-025-01683-w.

[19] Yang Y, He Q, Xia X, Dang Y, Chen X, He J, *et al*. Long-term functional prognosis and related factors of spinal cord stimulation in patients with disorders of consciousness. CNS Neuroscience & Therapeutics. 2022; 28: 1249–1258. https://doi.org/10.1111/cns.13870.

[20] Vorobyev AN, Varyukhina MD, Mayorova LA, Puzin KM, Radutnaya ML, Yakovlev AA, *et al*. The use of epidural spinal cord stimulation in patients with chronic disorders of consciousness - neuroimaging and clinical results. European Review for Medical and Pharmacological Sciences. 2023; 27: 681–686. https://doi.org/10.26355/eurrev_202301_31070.

[21] Huang W, Chen Q, Liu L, Tang J, Zhou H, Tang Z, *et al*. Clinical effect of short-term spinal cord stimulation in the treatment of patients with primary brainstem hemorrhage-induced disorders of consciousness. Frontiers in Neurology. 2023; 14: 1124871. https://doi.org/10.3389/fneur.2023.1124871.

[22] He Q, Yang C, Xu Y, Niu H, Wu H, Huang H, *et al*. Anatomical-related factors and outcome of percutaneous short-term spinal cord stimulation electrode shift in patients with disorders of consciousness: a retrospective study. Frontiers in Aging Neuroscience. 2024; 16: 1403156. https://doi.org/10.3389/fnagi.2024.1403156.

[23] Zhuang Y, Yang Y, Xu L, Chen X, Geng X, Zhao J, *et al*. Effects of short-term spinal cord stimulation on patients with prolonged disorder of consciousness: A pilot study. Frontiers in Neurology. 2022; 13: 1026221. https://doi.org/10.3389/fneur.2022.1026221.

[24] Wang Y, Dang Y, Bai Y, Xia X, Li X. Evaluating the effect of spinal cord stimulation on patient with disorders of consciousness: A TMS-EEG study. Computers in Biology and Medicine. 2023; 166: 107547. https://doi.org/10.1016/j.compbiomed.2023.107547.

[25] Vertes RP, Linley SB, Rojas AKP. Structural and functional organization of the midline and intralaminar nuclei of the thalamus. Frontiers in Behavioral Neuroscience. 2022; 16: 964644. https://doi.org/10.3389/fnbeh.2022.964644.

[26] Zhu Z, Hu X, Mao Y. Spinal cord electrical stimulation for severe disturbance of consciousness after traumatic brain injury: A case report. Heliyon. 2024; 10: e34913. https://doi.org/10.1016/j.heliyon.2024.e34913.

[27] Di Perri C, Bahri MA, Amico E, Thibaut A, Heine L, Antonopoulos G, *et al*. Neural correlates of consciousness in patients who have emerged from a minimally conscious state: a cross-sectional multimodal imaging study. The Lancet. Neurology. 2016; 15: 830–842. https://doi.org/10.1016/S1474-4422(16)00111-3.

[28] Zang YF, He Y, Zhu CZ, Cao QJ, Sui MQ, Liang M, *et al*. Altered baseline brain activity in children with ADHD revealed by resting-state functional MRI. Brain & Development. 2007; 29: 83–91. https://doi.org/10.1016/j.braindev.2006.07.002.

[29] Yu Y, Chen L, Wang Q, Hu L, Ding Q, Jia X, *et al*. Altered Amplitude of Low-Frequency Fluctuations in Inactive Patients with Nonneuropsychiatric Systemic Lupus Erythematosus. Neural Plasticity. 2019; 2019: 9408612. https://doi.org/10.1155/2019/9408612.

[30] Jia XZ, Sun JW, Ji GJ, Liao W, Lv YT, Wang J, *et al*. Percent amplitude of fluctuation: A simple measure for resting-state fMRI signal at single voxel level. PloS One. 2020; 15: e0227021. https://doi.org/10.1371/journal.pone.0227021.

[31] Chen X, Qin X, Zhuang Y, Li Z, Liang Z, Zhang H, *et al*. The Impact of Bispectral Index Monitoring on Outcomes in Spinal Cord Stimulation for Chronic Disorders of Consciousness. Ther-

apeutics and Clinical Risk Management. 2024; 20: 677–687. https://doi.org/10.2147/TCRM.S478489.

[32] Wang H, Hu Y, Ge Q, Dang Y, Yang Y, Xu L, *et al*. Thalamic burst and tonic firing selectively indicate patients' consciousness level and recovery. Innovation (Cambridge (Mass.)). 2025; 6: 100846. https://doi.org/10.1016/j.xinn.2025.100846.

[33] Chen X, Cramer SR, Chan DCY, Han X, Zhang N. Sequential Deactivation Across the Hippocampus-Thalamus-mPFC Pathway During Loss of Consciousness. Advanced Science (Weinheim, Baden-Wurttemberg, Germany). 2024; 11: e2406320. https://doi.org/10.1002/advs.202406320.

[34] Jang SH, Seo YS. Diffusion tensor tractography characteristics of axonal injury in concussion/mild traumatic brain injury. Neural Regeneration Research. 2022; 17: 978–982. https://doi.org/10.4103/1673-5374.324825.

[35] Graham NSN, Jolly A, Zimmerman K, Bourke NJ, Scott G, Cole JH, *et al*. Diffuse axonal injury predicts neurodegeneration after moderate-severe traumatic brain injury. Brain: a Journal of Neurology. 2020; 143: 3685–3698. https://doi.org/10.1093/brain/awaa316.

[36] Lu Y, Lin Z, Li M, Zhuang Y, Nie B, Lei J, *et al*. Three-phase Enriched Environment Improves Post-stroke Gait Dysfunction via Facilitating Neuronal Plasticity in the Bilateral Sensorimotor Cortex: A Multimodal MRI/PET Analysis in Rats. Neuroscience Bulletin. 2024; 40: 719–731. https://doi.org/10.1007/s12264-023-01155-1.

[37] Gao BY, Sun CC, Xia GH, Zhou ST, Zhang Y, Mao YR, *et al*. Paired associated magnetic stimulation promotes neural repair in the rat middle cerebral artery occlusion model of stroke. Neural Regeneration Research. 2020; 15: 2047–2056. https://doi.org/10.4103/1673-5374.282266.

[38] Hong W, Liu Z, Zhang X, Li M, Yu Z, Wang Y, *et al*. Distance-related functional reorganization predicts motor outcome in stroke patients. BMC Medicine. 2024; 22: 247. https://doi.org/10.1186/s12916-024-03435-7.

[39] Weis CN, Webb EK, deRoon-Cassini TA, Larson CL. Emotion Dysregulation Following Trauma: Shared Neurocircuitry of Traumatic Brain Injury and Trauma-Related Psychiatric Disorders. Biological Psychiatry. 2022; 91: 470–477. https://doi.org/10.1016/j.biopsych.2021.07.023.

[40] Zaghmi A, Pérez-Mato M, Dopico-López A, Candamo-Lourido M, Campos F, Gauthier MA. New Perspectives for Developing Therapeutic Bioconjugates of Metabolite-Depleting Enzymes: Lessons Learned Combating Glutamate Excitotoxicity. Biomacromolecules. 2022; 23: 1864–1872. https://doi.org/10.1021/acs.biomac.2c00117.

[41] Verma M, Lizama BN, Chu CT. Excitotoxicity, calcium and mitochondria: a triad in synaptic neurodegeneration. Translational Neurodegeneration. 2022; 11: 3. https://doi.org/10.1186/s40035-021-00278-7.

[42] Graham NSN, Cole JH, Bourke NJ, Schott JM, Sharp DJ. Distinct patterns of neurodegeneration after TBI and in Alzheimer's disease. Alzheimer's & Dementia. 2023; 19: 3065–3077. https://doi.org/10.1002/alz.12934.

[43] Kaplan GB, Leite-Morris KA, Wang L, Rumbika KK, Heinrichs SC, Zeng X, *et al*. Pathophysiological Bases of Comorbidity: Traumatic Brain Injury and Post-Traumatic Stress Disorder. Journal of Neurotrauma. 2018; 35: 210–225. https://doi.org/10.1089/neu.2016.4953.

[44] Poppa T, Benschop L, Horczak P, Vanderhasselt MA, Carrette E, Bechara A, *et al*. Auricular transcutaneous vagus nerve stimulation modulates the heart-evoked potential. Brain Stimulation. 2022; 15: 260–269. https://doi.org/10.1016/j.brs.2021.12.004.

[45] Pfeffer T, Keitel C, Kluger DS, Keitel A, Russmann A, Thut G, *et al*. Coupling of pupil- and neuronal population dynamics reveals diverse influences of arousal on cortical processing. eLife. 2022; 11: e71890. https://doi.org/10.7554/eLife.71890.

[46] Li Y, Li C, Chen QY, Hao S, Mao J, Zhang W, *et al*. Alleviation of migraine related pain and anxiety by inhibiting calcium-stimulating AC1-dependent CGRP in the insula of adult rats. The Journal of Headache and Pain. 2024; 25: 81. https://doi.org/10.1186/s10194-024-01778-3.

[47] Luo W, Yang Z, Zheng J, Cai Z, Li X, Liu J, *et al*. Small Molecule Hydrogels Loading Small Molecule Drugs from Chinese Medicine for the Enhanced Treatment of Traumatic Brain Injury. ACS Nano. 2024; 18: 28894–28909. https://doi.org/10.1021/acsnano.4c09097.

[48] Qin Z, Qu H, Liang HB, Zhou Q, Wang W, Wang M, *et al*. Altered resting-state effective connectivity of trigeminal vascular system in migraine without aura: A spectral dynamic causal modeling study. Headache. 2023; 63: 1119–1127. https://doi.org/10.1111/head.14602.

[49] Bianciardi M, Izzy S, Rosen BR, Wald LL, Edlow BL. Location of Subcortical Microbleeds and Recovery of Consciousness After Severe Traumatic Brain Injury. Neurology. 2021; 97: e113–e123. https://doi.org/10.1212/WNL.0000000000012192.

[50] De Oliveira Sergio T, Lei K, Kwok C, Ghotra S, Wegner SA, Walsh M, *et al*. The role of anterior insula-brainstem projections and alpha-1 noradrenergic receptors for compulsion-like and alcohol-only drinking. Neuropsychopharmacology: Official Publication of the American College of Neuropsychopharmacology. 2021; 46: 1918–1926. https://doi.org/10.1038/s41386-021-01071-w.

[51] Islam J, Rahman MT, Ali M, Kim HK, Kc E, Park YS. Optogenetic inhibition of ventrolateral orbitofrontal cortex astrocytes facilitates ventrolateral periaqueductal gray glutamatergic activity to reduce hypersensitivity in infraorbital nerve injury rat model. The Journal of Headache and Pain. 2025; 26: 41. https://doi.org/10.1186/s10194-025-01977-6.

[52] Olafson E, Russello G, Jamison KW, Liu H, Wang D, Bruss JE, *et al*. Frontoparietal network activation is associated with motor recovery in ischemic stroke patients. Communications Biology. 2022; 5: 993. https://doi.org/10.1038/s42003-022-03950-4.

[53] Esser F, Paul T, Rizor E, Binder E, Hensel L, Rehme AK, *et al*. Distinct Disconnection Patterns Explain Task-Specific Motor Impairment and Outcome After Stroke. Stroke. 2025; 56: 2210–2221. https://doi.org/10.1161/STROKEAHA.125.050929.

[54] Lee J, Chang WH, Chung JW, Kim SJ, Kim SK, Lee JS, *et al*. Efficacy of Intravenous Mesenchymal Stem Cells for Motor Recovery After Ischemic Stroke: A Neuroimaging Study. Stroke. 2022; 53: 20–28. https://doi.org/10.1161/STROKEAHA.121.034505.

[55] Mofakham S, Liu Y, Hensley A, Saadon JR, Gammel T, Cosgrove ME, *et al*. Injury to thalamocortical projections following traumatic brain injury results in attractor dynamics for cortical networks. Progress in Neurobiology. 2022; 210: 102215. https://doi.org/10.1016/j.pneurobio.2022.102215.

[56] Song D, Wang C, Jin Y, Deng Y, Yan Y, Wang D, *et al*. Mediodorsal thalamus-projecting anterior cingulate cortex neurons modulate helping behavior in mice. Current Biology: CB. 2023; 33: 4330–4342.e5. https://doi.org/10.1016/j.cub.2023.08.070.

[57] Carey G, Görmezoğlu M, de Jong JJA, Hofman PAM, Backes WH, Dujardin K, *et al*. Neuroimaging of Anxiety in Parkinson's Disease: A Systematic Review. Movement Disorders: Official Journal of the Movement Disorder Society. 2021; 36: 327–339. https://doi.org/10.1002/mds.28404.

[58] Ghulaxe Y, Joshi A, Chavada J, Huse S, Kalbande B, Sarda PP. Understanding Focal Seizures in Adults: A Comprehensive Review. Cureus. 2023; 15: e48173. https://doi.org/10.7759/cureus.48173.

[59] Gao J, Yang C, Li Q, Chen L, Jiang Y, Liu S, *et al*. Hemispheric

Difference of Regional Brain Function Exists in Patients With Acute Stroke in Different Cerebral Hemispheres: A Resting-State fMRI Study. Frontiers in Aging Neuroscience. 2021; 13: 691518. https://doi.org/10.3389/fnagi.2021.691518.

[60] Singh K, García-Gomar MG, Bianciardi M. Probabilistic Atlas of the Mesencephalic Reticular Formation, Isthmic Reticular Formation, Microcellular Tegmental Nucleus, Ventral Tegmental Area Nucleus Complex, and Caudal-Rostral Linear Raphe Nucleus Complex in Living Humans from 7 Tesla Magnetic Resonance Imaging. Brain Connectivity. 2021; 11: 613–623. https://doi.org/10.1089/brain.2020.0975.

[61] Guo C, Wang B, Huo Y, Shan L, Qiao T, Yang Z, *et al*. The effects of P2 segment of posterior cerebral artery to thalamus blood supply pattern on gait in cerebral small vessel disease: A 7 T MRI based study. Neurobiology of Disease. 2024; 190: 106372. https://doi.org/10.1016/j.nbd.2023.106372.

[62] Wang Y, You L, Tan K, Li M, Zou J, Zhao Z, *et al*. A common thalamic hub for general and defensive arousal control. Neuron. 2023; 111: 3270–3287.e8. https://doi.org/10.1016/j.neuron.2023.07.007.

[63] Acsády L, Mátyás F. Several ways to wake you up by the thalamus. Neuron. 2023; 111: 3140–3142. https://doi.org/10.1016/j.neuron.2023.09.020.

[64] Xue X, Wu JJ, Xing XX, Ma J, Zhang JP, Xiang YT, *et al*. Mapping individual cortico-basal ganglia-thalamo-cortical circuits integrating structural and functional connectome: implications for upper limb motor impairment poststroke. MedComm. 2024; 5: e764. https://doi.org/10.1002/mco2.764.

[65] Ramot A, Taschbach FH, Yang YC, Hu Y, Chen Q, Morales BC, *et al*. Motor learning refines thalamic influence on motor cortex. Nature. 2025; 643: 725–734. https://doi.org/10.1038/s41586-025-08962-8.

[66] Blumenfeld H. Arousal and Consciousness in Focal Seizures. Epilepsy Currents. 2021; 21: 353–359. https://doi.org/10.1177/15357597211029507.

[67] Steward T, Kung PH, Davey CG, Moffat BA, Glarin RK, Jamieson AJ, *et al*. A thalamo-centric neural signature for restructuring negative self-beliefs. Molecular Psychiatry. 2022; 27: 1611–1617. https://doi.org/10.1038/s41380-021-01402-9.

[68] Wolff M, Halassa MM. The mediodorsal thalamus in executive control. Neuron. 2024; 112: 893–908. https://doi.org/10.1016/j.neuron.2024.01.002.

[69] Zuo XN, Di Martino A, Kelly C, Shehzad ZE, Gee DG, Klein DF, *et al*. The oscillating brain: complex and reliable. NeuroImage. 2010; 49: 1432–1445. https://doi.org/10.1016/j.neuroimage.2009.09.037.

[70] Yang L, Yan Y, Wang Y, Hu X, Lu J, Chan P, *et al*. Gradual Disturbances of the Amplitude of Low-Frequency Fluctuations (ALFF) and Fractional ALFF in Alzheimer Spectrum. Frontiers in Neuroscience. 2018; 12: 975. https://doi.org/10.3389/fnins.2018.00975.